INTERNATIONAL JOURNAL OF
NUMERICAL ANALYSIS AND MODELING
Volume 15, Number 1-2, Pages 74–85

MODELING AND SIMULATION OF THE ATMOSPHERIC DUST DYNAMIC: FRACTIONAL CALCULUS AND CLOUD COMPUTING

LUIS VÁZQUEZ[1*], M. PILAR VELASCO[2], JOSÉ LUIS VÁZQUEZ-POLETTI[1†], IGNACIO M. LLORENTE[1†], DAVID USERO[1*], AND SALVADOR JIMÉNEZ[2]

This paper is dedicated to Professor Benyu Guo

Abstract. The dust aerosols have an important effect on the solar radiation in the Martial atmosphere and both surface and atmospheric heating rates, which are also basic drivers of atmospheric dynamics. Aerosols cause an attenuation of the solar radiation traversing the atmosphere and this attenuation is modeled by the Lambert-Beer-Bouguer law, where the aerosol optical thickness plays an important role. Through Angstrom law, the aerosol optical thickness can be approximated and this law allows to model attenuation of the solar radiation traversing the atmosphere by a fractional diffusion equation. The analytical solution is available in the case of one space dimension. When we extend the fractional diffusion equation to the case of two or more space variables, we need large and massive computations to approach numerically the solutions. In this case a suitable strategy is to use the cloud computing to carry out the simulations. We present an introduction to cloud computing applied to the fractional diffusion equation in one dimension.

Key words. Dust, solar radiation, fractional calculus, Mittag-Leffler type functions, fractional ordinary and partial differential equations, cloud computing, performance model, cost model

1. Introduction

Aerosols are minute particles suspended in the atmosphere which can scatter and absorb sunlight if they are sufficiently large. Thus, the aerosols interact both directly and indirectly with the Earth's radiation budget and climate. A direct effect of the interaction of the aerosols with the Sun radiation and climate is that the aerosols scatter sunlight directly back into space. By other hand, the aerosols in the lower atmosphere can modify indirectly the size of cloud particles, changing how the clouds reflect and absorb sunlight, thereby affecting the energy budget of the planet.

The dust particles are a type of aerosol with a significant effect on climate, because the dust is composed of particles of minerals that absorb sunlight as well as scatter it. By absorbing sunlight, the dust particles warm the layer of the atmosphere where they reside and this could inhibit the formation of storm clouds and expand the desert scenario.

In the particular case of the Martian atmosphere, the dust aerosols have an important effect on the solar radiation and both surface and atmospheric heating rates, which are also basic drivers of atmospheric dynamics. The importance of the dust in the martian exploration was recognized early in 1972 and since then dust is a target of atmospheric studies ([1], [2], [3]).

Under different Martian atmospheric scenarios, the measure of the amount of solar radiation at the Martian surface will be useful to gain some insight into the following issues:

Received by the editors January 25, 2017 and, in revised form, April 4, 2017.
2000 *Mathematics Subject Classification.* 26A33, 33E12, 34A08, 34K37, 35R11, 60G22, 68U01, 68M01, 68M20.

1) UV irradiation levels at the bottom of the Martian atmosphere to use them as an habitability index.
2) Incoming shortwave radiation and solar heating at the surface.
3) Relative local index of dust in the atmosphere.

Principally, the dust aerosols cause an attenuation of the solar radiation traversing the atmosphere. This attenuation is modeled by the Lambert-Beer-Bouguer law, where the aerosol optical thickness plays an important role and, through Angstrom law, the aerosol optical thickness can be approximated. However, the classical model often does not fit to the reality since the propagation of the solar radiation in the atmosphere is a complex process, whose dynamic is governed by different time/space scales. Thus, it is natural to think about integro-differential equations to describe a better modeling.

In this point, the Fractional Calculus offers new scenarios of modeling, since the fractional derivatives and integrals are non-local and they involve convolution kernels which act as memory factors. These properties make that the Fractional Calculus offers more suitable models to describe many physical phenomena, for instance, the dynamic of the martian atmosphere. Specifically, the attenuation of the solar radiation traversing the atmosphere can be modeled more accurately by a fractional diffusion equation, which provides a generalization of the classical Angstrom law.

This paper is organized as follow. In Section 2, we explain the fundamental laws that model the propagation of the solar radiation in a medium, and the basic elements of Fractional Calculus that we will use are introduced in Section 3. Next, in Section 4 the physics laws are reinterpreted in terms of Fractional Calculus and a new fractional model is obtained for the dynamic of the attenuation of the solar radiation traversing the martian atmosphere. In Section 5 we consider the numerical algorithms for one and two space dimensions. The associated simulations for one space dimension are described in section 6 and in the framework of the cloud computing. In this moment, we are applying the above computational strategy to the two dimensional case and the results will be published soon. Finally in section 6 we describe the cloud computing strategy and we implement it for the one dimensional fractional equation.

2. Foundations of the propagation of a radiation in a medium

2.1. Attenuation of the radiation. In the study of the propagation of the solar radiation in a medium, it is fundamental to know the attenuation of solar radiation traversing the atmosphere ([4], [5]). This attenuation is modeled by the Lambert-Beer-Bouguer law:

Definition 1. ***The Lambert-Beer-Bouguer law*** *establishes that the direct solar irradiance $F(\lambda)$ at the Mars's surface at wavelength λ is given by*

$$F(\lambda) = DF_0(\lambda)e^{-\tau(\lambda)m}, \tag{1}$$

where $F_0(\lambda)$ is the spectral irradiance at the top of the atmosphere, m is the absolute air mass, D is the correction factor for the earth-sun distance, and $\tau(\lambda)$ is the total optical thickness at wavelength λ.

2.2. Relevance of the aerosol optical thickness. The total optical thickness is obtained as the sum of the molecular scattering optical thickness $\tau_r(\lambda)$, the absorption optical thickness for atmospheric gases (O_2, O_3, H_2O, CO_2...) $\tau_g(\lambda)$, and the aerosol optical thickness $\tau_a(\lambda)$. In particular, $\tau_a(\lambda)$ can be obtained by direct solar spectral irradiance measurements by following the Angstrom Law [6]

Proposition 1. *According to the* ***Angstrom Law****, the aerosol optical thickness can be approximated over a limited wavelength range by the relation*

$$\tau_a^{-1} = \frac{\lambda^\alpha}{\beta}, \tag{2}$$

where α and β are parameters related to the size and the content of the aerosol, according to the following statements:

- *α is the parameter closely correlated to the size distribution of the scattering particles, and*
- *β is the extinction coefficient corresponding to a 1 μm wavelength, which depends on the concentration of aerosols in the atmosphere.*

In the particular case of the Martian solar irradiance, simulations of its radiative transfer have been obtained in [5] for $\alpha = 1.2$ and $\beta = 0.3$, corresponding to an aerosol optical thickness $\tau_a = 0.6$:

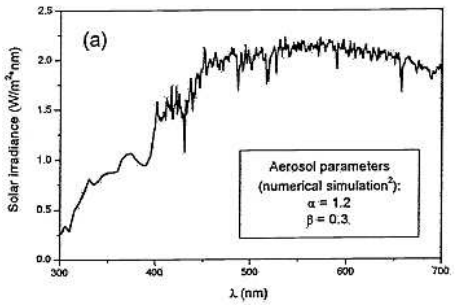

FIGURE 1. Example.

3. Elements of Fractional Calculus

There exist several definitions of fractional integral and derivative operators ([7], [8], [9], [10]): Riemman-Liouville, Liouville, Caputo, Grünwald-Letnikov... These operators generalize the ordinary concepts of derivatives and integrals from integer orders to non-integer orders and they return to the classical operators for integer orders. The existence of different definitions of fractional operators allows to obtain a wide spectrum of possibilities to model real phenomena. Also, it allows to consider a natural interpolation between diffusion and wave propagation models ([11], [12], [13]).

In this paper we will use the definition of the Caputo fractional derivative.

Definition 2. *Let $\alpha > 0$, with $n - 1 < \alpha < n$ and $n \in \mathbb{N}$, let D be the usual differential operator and let f be a suitable real function (for example, it suffices if $f \in L_1(\mathbb{R})$). The* ***Caputo fractional derivative*** *is:*

$$\frac{\partial^\alpha}{\partial t^\alpha} f(t) = \frac{1}{\Gamma(n-\alpha)} \int_0^x (t-s)^{n-\alpha-1} D^n f(s)\, ds \qquad t > 0, \alpha > 0. \tag{3}$$

This fractional derivative returns to the classical derivative for integer values of the parameter α,

$$\lim_{\alpha \to 0} (\frac{\partial^\alpha}{\partial t^\alpha} f)(t) = f(t), \tag{4}$$

$$(\frac{\partial^\alpha}{\partial t^\alpha} f)(t) = \frac{d^n}{dt^n} f(t), \tag{5}$$

and the Caputo fractional derivative of a constant is zero,

$$\frac{\partial^\alpha}{\partial t^\alpha} f(1) = 0. \tag{6}$$

However, the Caputo fractional derivative is not commutative in general, that is, this definition does not verify the derivatives algebra.

Property 1. *Let $n-1 < \alpha < n$, $m, n \in \mathbb{N}$, $\alpha \in \mathbb{R}$, and the function f is such that $\frac{\partial^\alpha}{\partial t^\alpha} f(t)$ exists. Then in general,*

$$\frac{\partial^\alpha}{\partial t^\alpha} \frac{\partial^m}{\partial t^m} f(t) = \frac{\partial^{\alpha+m}}{\partial t^{\alpha+m}} f(t) \neq \frac{\partial^m}{\partial t^m} \frac{\partial^\alpha}{\partial t^\alpha} f(t). \tag{7}$$

An important property of the Caputo fractional derivative is its relation with the Laplace transform $\mathcal{L}$.

Property 2. *Let $\alpha > 0$, $n-1 < \alpha \leq n$ $(n \in \mathbb{N})$ and $f \in C^n(\mathbb{R}^+)$ such that $f^{(n)}(t) \in L_1(0,b), \forall b > 0$, then:*

$$(\mathcal{L}\frac{\partial^\alpha}{\partial t^\alpha} f)(t) = t^\alpha (\mathcal{L}f)(t) - \sum_{k=0}^{n-1} t^{\alpha-k-1} (D^k f)(0). \tag{8}$$

In particular, for $0 < \alpha \leq 1$,

$$(\mathcal{L}\frac{\partial^\alpha}{\partial t^\alpha} f)(t) = t^\alpha (\mathcal{L}f)(t) - t^{\alpha-1} f(0). \tag{9}$$

Also, we remark that the Caputo fractional derivative verifies the following important relation:

Property 3.

$$\frac{\partial^\alpha}{\partial t^\alpha} E_\alpha(\lambda t^\alpha) = \lambda E_\alpha(\lambda t^\alpha), \qquad \alpha > 0, \lambda \in \mathbb{C}, \tag{10}$$

*where $E_\alpha(z) = \sum_{k=0}^{\infty} \frac{z^k}{\Gamma(\alpha k + 1)}$ is known as **Mittag-Leffler function**, which generalizes the classical exponential function.*

4. Different modeling scenarios

A classical diffusion process is modeled by the well-known diffusion equation

$$\frac{\partial \varphi}{\partial t} = c \frac{\partial^2 \varphi}{\partial x^2}, \tag{11}$$

where we have

$$\int_{-\infty}^{\infty} \varphi dx = 1, \tag{12}$$

and

$$\frac{d}{dt} < X^2 >= \int_{-\infty}^{\infty} x^2 \varphi_t dx = \int_{-\infty}^{\infty} x^2 c \varphi_{xx} dx = 2c, \tag{13}$$

from which we obtain the classical mean square value, associated to the Brownian motion,

$$< X^2 >= \int_{-\infty}^{\infty} x^2 \varphi dx = 2ct. \tag{14}$$

This approach is suitable for normal processes and homogeneous media. However, in many complex processes related to heterogeneous media or anomalous behavior, the mean square value could take a non-linear time dependence as

$$< X^2 >= \int_{-\infty}^{\infty} x^2 \varphi dx = 2ct^{\alpha}, \tag{15}$$

which justifies, in a deterministic way, the consideration of a time-fractional diffusion equation in many complex situations:

$$\frac{\partial^{\alpha}\varphi}{\partial t^{\alpha}} = c\frac{\partial^2 \varphi}{\partial x^2}. \tag{16}$$

Similar deterministic approaches have been deeply studied in the literature, for example [14], [15], [16], [17].

4.1. Wavelength-fractional diffusion equation. The propagation of the solar radiation in the atmosphere is a complex process. The dynamics is governed by different time/space scales. Thus, it is natural to think about integro-differential equations to describe a better modeling. In this context, we assume the following:

$$\frac{\partial^{\alpha}\varphi}{\partial \lambda^{\alpha}} = \frac{\Gamma(\alpha+1)}{2\beta}\frac{\partial^2 \varphi}{\partial x^2}, \qquad 0 < \alpha < 2. \tag{17}$$

$$\begin{cases} \lim\limits_{x\to\pm\infty} \varphi(\lambda, x) = 0, & \lambda > 0 \\ \varphi(0+, x) = \delta(x), & x \in \mathbb{R}, \\ \dfrac{\partial}{\partial \lambda}\varphi(\lambda, x)\Big|_{\lambda=0} = 0 & \text{(condition for } 1 < \alpha < 2\text{)}. \end{cases} \tag{18}$$

Their exact solution is known as fundamental solution or Green function, and it is expressed through the Mittag-Leffler and Wright functions:

$$\varphi(\lambda, x) = \frac{1}{2\pi}\int_{-\infty}^{\infty} E_{\alpha}\left(-\frac{\Gamma(\alpha+1)}{2\beta}\lambda^{\alpha}\right) e^{-ikx} dk \tag{19}$$

$$= \frac{1}{2\pi\lambda^{\alpha/2}} W\left(-\frac{|x|}{\lambda^{\alpha/2}}\left(\frac{\Gamma(\alpha+1)}{2\beta}\right)^{-1/2}; -\frac{\alpha}{2}; 1-\frac{\alpha}{2}\right). \tag{20}$$

4.2. Second and higher order moments. For this equation, their second order moment is

$$< X^2 >= \int_{-\infty}^{\infty} x^2 \varphi(t, x) dx = \frac{1}{\beta}\lambda^{\alpha}, \tag{21}$$

and we can obtain their high order moments (which could be measured) as

$$< X^{2n} >= \int_{-\infty}^{\infty} x^{2n}\varphi(\lambda, x) dx = \frac{\Gamma(2n+1)}{\Gamma(\alpha n+1)}\left(\frac{\Gamma(\alpha+1)}{2\beta}\lambda^{\alpha}\right)^n, \qquad n = 0, 1, 2... \tag{22}$$

4.3. Same situation under different conditions. It is possible to consider that the same aerosol optical thickness at each wavelength could be obtained under different conditions of diffusion and/or the size of the scattering particles. That is, from (2),

$$\frac{2c_1}{\Gamma(\alpha_1+1)}\lambda^{\alpha_1} = \frac{2c_2}{\Gamma(\alpha_2+1)}\lambda^{\alpha_2}, \tag{23}$$

and thus, we could obtain a relation

$$\lambda = \left(\frac{c_2\Gamma(\alpha_1+1)}{c_1\Gamma(\alpha_2+1)}\right)^{\frac{1}{\alpha_1-\alpha_2}}. \tag{24}$$

4.4. Relation between two aerosols. Let us consider two aerosols with aerosol optical thickness $\tau_{a,1}$ and $\tau_{a,2}$, characterized by α_1, β_1 and α_2, β_2, respectively. For each one, the diffusion process is determined by the equation (17) and then:

- The relation between theirs aerosol optical thickness is:

$$\frac{\tau_{a,2}}{\tau_{a,1}} = \frac{\beta_2}{\beta_1}\lambda^{\alpha_1-\alpha_2}. \tag{25}$$

- The relation between theirs diffusion coefficients is:

$$\frac{c_2}{c_1} = \frac{\Gamma(\alpha_2+1)\beta_2}{\Gamma(\alpha_1+1)\beta_1}. \tag{26}$$

5. Numerical approximations

5.1. Quadrature map of numerical integration. By using Caputo fractional derivative, the equation $\frac{\partial^\alpha \varphi}{\partial \lambda^\alpha} = f(\lambda)$, $0 < \alpha \leq 1$, is equivalent to $\varphi(\lambda) = \varphi(0) + I^\alpha f(\lambda)$, where I^α is the known Riemann-Liouville fractional integral of order α:

$$I^\alpha f(\lambda) = \frac{1}{\Gamma(\alpha)}\int_0^\lambda (\lambda-\tau)^{\alpha-1} f(\tau)d\tau, \quad 0 < \alpha \leq 1. \tag{27}$$

Thus, the equation (17) becomes:

$$\varphi(\lambda,x) = \varphi(0,x) + \frac{1}{\Gamma(\alpha)}\int_0^\lambda (\lambda-\tau)^{\alpha-1}\frac{\Gamma(\alpha+1)}{2\beta}\frac{\partial^2\varphi}{\partial x^2}(\lambda,x)d\tau, \quad 0 < \alpha \leq 1. \tag{28}$$

Now, by approaching the integral with a map, we obtain the following scheme (see [18]):

$$\varphi(\lambda_n,x) = \varphi(0,x) + \frac{\alpha}{2\beta}\sum_{k=0}^{n-1}\frac{\partial^2\varphi}{\partial x^2}(\lambda_k,x)\int_{k\Delta\lambda}^{(k+1)\Delta\lambda}(n\Delta\lambda-\tau)^{\alpha-1}d\tau, \quad 0 < \alpha \leq 1, \tag{29}$$

and, after evaluating the integral the scheme reads

$$\varphi(\lambda_n,x) = \varphi(0,x) + \frac{(\Delta\lambda)^\alpha}{2\beta}\sum_{k=0}^{n-1}\frac{\partial^2\varphi}{\partial x^2}(\lambda_k,x)[(n-k)^\alpha - (n-k-1)^\alpha], \quad 0 < \alpha \leq 1. \tag{30}$$

5.2. Approximations for two spatial dimensions. A analysis of quadrature map of numerical integration similar to the previous subsection can be obtained if we consider the equation with two spatial dimensions:

$$\frac{\partial^\alpha\varphi}{\partial\lambda^\alpha} = \frac{\Gamma(\alpha+1)}{2\beta}\left(\frac{\partial^2\varphi}{\partial x^2} + \frac{\partial^2\varphi}{\partial y^2}\right), \qquad 0 < \alpha \leq 1.$$

In this case, the resultant scheme is:

$$\begin{aligned}\varphi(\lambda_n,x,y) =& \varphi(0,x,y) + \frac{(\Delta\lambda)^\alpha}{2\beta}\sum_{k=0}^{n-1}\left(\frac{\partial^2\varphi}{\partial x^2} + \frac{\partial^2\varphi}{\partial y^2}\right)\\ &\times(\lambda_k,x,y)[(n-k)^\alpha - (n-k-1)^\alpha], \quad 0 < \alpha \leq 1.\end{aligned} \tag{31}$$

By the other hand, an accuracy implicit difference approximation for the two dimensional time fractional diffusion equation was introduced by Zhuang and Liu in

[19] and this scheme can be applyed to the wavelength-fractional diffusion equation with two spatial dimensions,

$$\frac{\partial^\alpha \varphi}{\partial \lambda^\alpha} = \frac{\Gamma(\alpha+1)}{2\beta}\left(\frac{\partial^2 \varphi}{\partial x^2} + \frac{\partial^2 \varphi}{\partial y^2}\right), \qquad 0 < \alpha \leq 1,$$

with initial and boundary conditions

$$\begin{aligned} &\varphi(0,x,y) = f(x,y), \quad (x,y) \in \Omega, \\ &\varphi(\lambda,x,y)|_{\delta\Omega} = 0, \qquad 0 \leq \lambda \leq T, \end{aligned} \tag{32}$$

where $\Omega = \{(x,y)|x \in [0,L], y \in [0,M]\}$.

Let us define

$$\begin{aligned} &\lambda_k = k\tau, \quad k = 0,1,2,\ldots,n, \quad \tau = \frac{T}{n}, \\ &x_i = i\Delta x, \quad i = 0,1,2,\ldots,l, \quad \Delta x = \frac{L}{i}, \\ &y_j = j\Delta y, \quad j = 0,1,2,\ldots,m, \quad \Delta y = \frac{M}{m}. \end{aligned} \tag{33}$$

Then we can obtain the following numerical approximation for $\varphi_{i,j}^k = \varphi(\lambda_k, x_i, y_j)$:

$$\begin{aligned} &\varphi_{i,j}^{k+1} - \varphi_{i,j}^k + \sum_{s=1}^{k}((s+1)^{1-\alpha} - s^{1-\alpha})(\varphi_i^{k+1-s} - \varphi_i^{k-s}) = \frac{\Gamma(\alpha+1)}{2\beta}\tau^\alpha \Gamma(2-\alpha) \\ &\left(\frac{\varphi_{i+1,j}^{k+1} - 2\varphi_{i,j}^{k+1} + \varphi_{i-1,j}^{k+1}}{(\Delta x)^2} + \frac{\varphi_{i,j+1}^{k+1} - 2\varphi_{i,j}^{k+1} + \varphi_{i,j-1}^{k+1}}{(\Delta y)^2}\right) \end{aligned} \tag{34}$$

According the fractional derivatives algebra is not possible to factorize the solutions and as a consequence the numerical simulations need large and massive computations. The possible scenario for such simulations is the cloud computing environment which is introduced in the next section for the one dimensional case.

6. Computational work

A one-dimensional case was implemented in Octave[1] and two sets of experiments were considered by varying the values of x and λ:

- **A set:** $\lambda = 1:1:2, x = 0:0.1:n$
- **B set:** $\lambda = 1:1:n, x = 0:0.1:1$

being n increased at each experiment.

Due to the computational requirements of the code, cloud computing was considered for providing the necessary resources in order to obtain a reasonable execution time and monetary cost. The following subsections explain the porting of the code to this computing paradigm, some experimental results and the fostering of an execution model that allows to obtain the best setup by means of performance (execution time) and cost.

6.1. Cloud computing infrastructure. A public cloud infrastructure like that offered by Amazon Web Services[2] was used for the porting of the code. These kind of infrastructures not only provide a dynamic, elastic and on demand provision of computational resources [20, 21, 22], but also a "pay-as-you-go" fashion which makes this solution in many scientific scenarios [23, 24].

Amazon EC2 offers solutions at the IaaS (Infrastructure as a Service) level. Here, the user has a wide variety of virtual machines or instances to choose from

[1] https://www.gnu.org/software/octave/

[2] https://aws.amazon.com/ec2/

TABLE 1. Instances from Amazon EC2 used in this work and their hourly prices.

Instance	CPUs	Memory	Price/hour
t2.small	1	2GB	$0.026
c4.large	2	3.75GB	$0.105

by means of elements such the number of CPUs and the memory size. Table 1 shows the characteristics of the two instance types used during the experiments along with their hourly prices.

As for the software, Ubuntu 16.04 was chosen as the operative system and Octave was installed from the official repositories.

6.2. Experiments. Aside from the sets of experiments described at the beginning of this Section, three sets of executions were considered taking into account the number of CPUs and the level of parallelization:

- **t2.small:** using the *t2.small* instance and running the code on its only CPU.
- **c4.large 1CPU:** using the *c4.large* instance and using its two CPU for running the code.
- **c4.large 2CPU:** using the *c4.large* instance but running two copies of the code in parallel simulating half of the interval each.

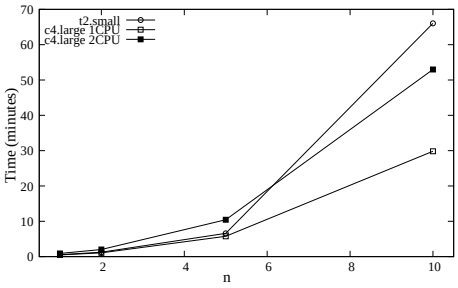

FIGURE 2. Experimental results for the A set.

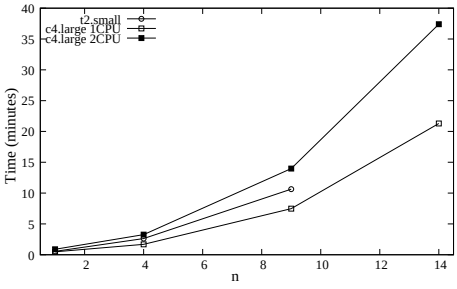

FIGURE 3. Experimental results for the B set. Execution time in *t2.small* for $n \geq 9$ is not deterministic.

Figure 2 shows the execution results for the A experiment set ($\lambda = 1 : 1 : 2, x = 0 : 0.1 : n$). It can be seen that bot *t2.small* and *c4.large 1CPU* behave

similarly until the interval (n) exceeds the 5 value. Both parallelization strategies with c4.large seem to better that using the other instance.

However, it can be seen that allocating two "half" tasks on each *c4.large*'s CPUs doesn't increase the performance. This is because both tasks compete for shared resources such as memory.

A different behavior is shown in Figure 3, where execution results for the B experiment set ($\lambda = 1 : 1 : n, x = 0 : 0.1 : 1$) can be seen. This particular interval makes the *t2.small* instance inadequate for n values greater than 9, as machine resources are insufficient causing execution time to be not deterministic. On the other hand, the increase in execution time using the *c4.large 2CPU* strategy appears from the very beginning of the experiments.

6.3. Execution and cost model. From the experimental results described in the previous subsection a model con be fostered in order to obtain an optimal infrastructure setup by means of execution time or cost [25].

6.3.1. A experiment set. These are the equations that allow to estimate the execution time (y) of this set based on the studied interval (n) for the x value:

$$\text{t2.small: } y = 0.1108n^3 - 0.6193n^2 + 1.7873n - 0.7275 \tag{35}$$

$$\text{c4.large 1CPU: } y = 0.0185n^3 + 0.0926n^2 + 0.1924n + 0.1704 \tag{36}$$

$$\text{c4.large 2CPU: } y = 0.0322n^3 + 0.1649n^2 + 0.3969n + 0.306 \tag{37}$$

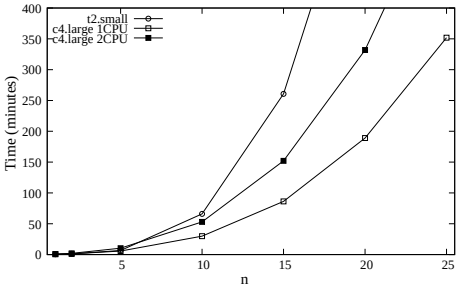

FIGURE 4. Execution time model for the A experiment set.

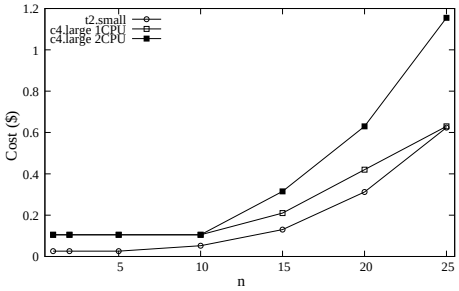

FIGURE 5. Cost model for the A experiment set.

Figure 4 represents a set of values for this model and Figure 5 shows the correspondent cost. As Amazon EC2 charges for whole hours, execution time is rounded and then multiplied to the hourly price shown in Table 1.

Considering costs, *t2.small* and specially *c4.large 1CPU* are the best options if there is no strict deadline for the simulations. Even, while $n \leq 25$, *t2.small* turns to be the most convenient instance type.

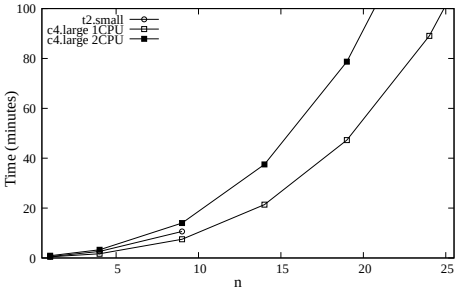

FIGURE 6. Execution time model for the B experiment set.

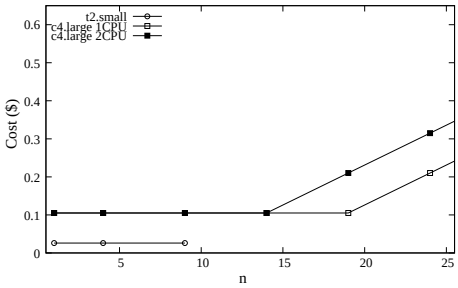

FIGURE 7. Cost model for the B experiment set.

6.3.2. B experiment set. The execution time (y) of this set based on the studied interval (n) for the x value can be estimated by the following equations:

$$\text{t2.small: } y = 0.1142n^2 + 0.1188n + 0.3183, n \leq 9 \tag{38}$$

$$\text{c4.large 1CPU: } y = 0.0052n^3 + 0.0214n^2 + 0.1909n + 0.2565 \tag{39}$$

$$\text{c4.large 2CPU: } y = 0.0066n^3 + 0.077n^2 + 0.2686n + 0.5416 \tag{40}$$

Figures 6 and 7 show both the execution time and cost model for this experiment data set.

An interesting feature is that while *c4.large 1CPU* offers the best performance, there is no difference of price with *c4.large 2CPU* for $n \leq 14$. Also, the execution time difference between both *c4.large* strategies increases with n, something that does not apply to the cost. Finally, *t2.small* is a balanced option for a low n value (9).

Acknowledgments

The authors thank to the support of MINECO of Spain, through the project ESP2016-79135-R, TIN2015-65469-P and the special support from the University Francisco de Vitoria (Madrid).

References

[1] P. Gierasch and R. Goody, "The effect of dust on the temperature of the martian atmosphere," J. Atmos. Sci., vol. 29, pp. 400 – 402, 1972.

[2] M. Lemmon, M. Wolff, J. Bell, M. Smith, B. Cantor, and P. Smith, "Dust aerosol, clouds, and the atmospheric optical depth record over 5 mars years of the mars exploration rover mission," Icarus, vol. 251, pp. 96 – 111, 2015.

[3] M. Smith, "Spacecraft observations of the martian atmosphere," Ann. Rev. Earth Planet. Sci., vol. 36, pp. 191 – 219, 2008.

[4] V. Cachorro, A. de Frutos, and J. Casanova, "Determination of the angstrom turbidity parameters," Applied Optics, vol. 26, no. 15, pp. 3069 – 3076, 1987.

[5] C. Córdoba and L. Vázquez, "Characterization of atmospheric aerosols by an in-situ photometric technique in planetary environments," in First Jet Propulsion Laboratory In Situ Instruments Workshop, SPIE, vol. 4878, 2003.

[6] A. Angstrom, "On the atmospheric transmission of sun radiation and on dust in the air," Geografiska Annaler, vol. 11, pp. 156 – 166, 1929.

[7] K. Diethelm, The analysis of fractional differential equations. New York: Springer, 2010.

[8] A. Kilbas, H. Srivastava, and J. Trujillo, Theory and Applications of Fractional Differential Equations. Amsterdam: Elsevier, 2006.

[9] G. Zaslavsky, D. Baleanu, and J. Tenreiro, Fractional Differentiation and its Applications. Physica Scripta, 2009.

[10] L. Vázquez and H. Jafari(eds.), "Fractional calculus: theory and numerical methods," Central European Journal of Physics, vol. 11, no. 10, 2013.

[11] L. Vázquez and M. Velasco, "Aplicación del cálculo fraccionario a los procesos de relajación," Memorias de la Real Academia de Ciencias Exactas, Fsicas y Naturales. Serie de Ciencias Exactas, vol. Tomo XXXV. Cálculo Fraccionario, Fractales y Aplicaciones, pp. 105 – 115, 2009.

[12] M. Velasco and L. Vázquez, "On the fractional newton and wave equation in one space dimension," Applied Mathematical Modeling, no. 38, pp. 3314 – 3324, 2014.

[13] M. Velasco, D. Usero, S. Jiménez, C. Aguirre, and L. Vázquez, "Mathematics and mars exploration," Pure and Applied Geophysics, vol. 172, pp. 33 – 47, 2015.

[14] R. Gorenflo and F. Mainardi, "Random walk models for space fractional diffusion processes," Fractional Calculus and Applied Analysis, no. 1, pp. 167 – 191, 1998.

[15] R. Metzler and J. Klafter, "The random walk's guide to anomalous diffusion: a fractional dynamics approach," Physics Reports, no. 339, pp. 1 – 77, 2000.

[16] R. Gorenflo, F. Mainardi, D. Moretti, and P. Paridisi, "Time fractional diffusion: A discrete random walk approach," Nonlinear Dynamics, no. 29, pp. 129 – 143, 2002.

[17] R. Klages, G. Radons, and I. Sokolov, Eds., Anomalous Transport: Foundations and Applications. United Kingdom: Wiley, 2008, ch. 4. Continuous Time Random Walk, Mittag-Leffler Waiting Time and Fractional Diffusion: Mathematical Aspects - R. Gorenflo and F. Mainardi.

[18] G. Turchetti, D. Usero, and L. Vázquez, "Hamiltonian systems with fractional time derivative," Tamsui Oxford J. Math. Sci., vol. 18, no. 1, pp. 31 – 44, 2002.

[19] P. Zhuang and F. Liu, "Finite difference approximation for two-dimensional time fractional diffusion equation," Journal of Algorithms and Computational Technology, vol. 1, no. 1, pp. 1 – 15, 2007.

[20] P. M. Mell and T. Grance, "Sp 800-145. the nist definition of cloud computing," Gaithersburg, MD, United States, Tech. Rep., 2011.

[21] M. Armbrust, A. Fox, R. Griffith, A. D. Joseph, R. Katz, A. Konwinski, G. Lee, D. Patterson, A. Rabkin, I. Stoica, and M. Zaharia, "A view of cloud computing," Commun. ACM, vol. 53, no. 4, pp. 50–58, Apr. 2010.

[22] Y. Jadeja and K. Modi, "Cloud computing - concepts, architecture and challenges," in 2012 International Conference on Computing, Electronics and Electrical Technologies (ICCEET), March 2012, pp. 877–880.

[23] J. L. Vázquez-Poletti, D. Santos-Muñoz, I. M. Llorente, and F. Valero, "A cloud for clouds: Weather research and forecasting on a public cloud infrastructure," in Cloud Computing and Services Sciences - International Conference in Cloud Computing and Services Sciences, CLOSER 2014, Barcelona Spain, April 3-5, 2014, Revised Selected Papers, 2014, pp. 3–11.

[24] J. Vázquez-Poletti, R. Moreno-Vozmediano, R. Han, W. Wang, and I. Llorente, "Saas enabled admission control for {MCMC} simulation in cloud computing infrastructures," Computer Physics Communications, vol. 211, pp. 88 – 97, 2017, high Performance Computing for Advanced Modeling and Simulation of Materials.

[25] G. D. Guerrero, R. M. Wallace, J. L. Vázquez-Poletti, J. M. Cecilia, J. M. García, D. Mozos, and H. E. P. Sánchez, "A performance/cost model for a CUDA drug discovery application on physical and public cloud infrastructures," Concurrency and Computation: Practice and Experience, vol. 26, no. 10, pp. 1787–1798, 2014. [Online].

[1*]Department of Applied Mathematics and [1†]Department of Computer Architecture and Automatics, Universidad Complutense de Madrid, Madrid, Spain

E-mail: lvazquez@fdi.ucm.es and jlvazquez@fdi.ucm.es and llorente@dacya.ucm.es and umdavid@mat.ucm.es

[2]Department of Applied Mathematics to Information and Communication Technologies, Universidad Politécnica de Madrid, Madrid, Spain

E-mail: mp.velasco@upm.es and s.jimenez@upm.es